



5-6-2019

A Climatology of Atmospheric Patterns Associated with Red River Valley Blizzards

Aaron Kennedy

University of North Dakota, aaron.kennedy@UND.edu

Alexander Trellinger

Thomas Grafenauer

Gregory Gust

Follow this and additional works at: <https://commons.und.edu/as-fac>

Recommended Citation


Kennedy, Aaron; Trellinger, Alexander; Grafenauer, Thomas; and Gust, Gregory, "A Climatology of Atmospheric Patterns Associated with Red River Valley Blizzards" (2019). *Atmospheric Sciences Faculty Publications*. 6.

<https://commons.und.edu/as-fac/6>

This Article is brought to you for free and open access by the Department of Atmospheric Sciences at UND Scholarly Commons. It has been accepted for inclusion in Atmospheric Sciences Faculty Publications by an authorized administrator of UND Scholarly Commons. For more information, please contact zeineb.yousif@library.und.edu.

Article

A Climatology of Atmospheric Patterns Associated with Red River Valley Blizzards

Aaron Kennedy ^{1,*}, Alexander Trellinger ², Thomas Grafenauer ³ and Gregory Gust ³¹ Department of Atmospheric Sciences, University of North Dakota, Grand Forks, ND 58202, USA² NOAA/National Weather Service, Sioux Falls, SD 57104, USA; alex.trellinger@noaa.gov³ NOAA/National Weather Service, Grand Forks, ND 58203, USA; thomas.grafenauer@noaa.gov (T.G.); gregory.gust@noaa.gov (G.G.)

* Correspondence: aaron.kennedy@und.edu; Tel.: +1-701-777-5269

Received: 12 March 2019; Accepted: 1 May 2019; Published: 6 May 2019



Abstract: Stretching along the border of North Dakota and Minnesota, The Red River Valley (RRV) of the North has the highest frequency of reported blizzards within the contiguous United States. Despite the numerous impacts these events have, few systematic studies exist that discuss the meteorological properties of blizzards. As a result, forecasting these events and lesser blowing snow events is an ongoing challenge. This study presents a climatology of atmospheric patterns associated with RRV blizzards for the winter seasons of 1979–1980 and 2017–2018. Patterns were identified using subjective and objective techniques using meteorological fields from the North American Regional Re-analysis (NARR). The RRV experiences, on average, 2.6 events per year. Blizzard frequency is bimodal, with peaks occurring in December and March. The events can largely be typed into four meteorological categories dependent on the forcing that drives the blizzard: Alberta Clippers, Arctic Fronts, Colorado Lows, and Hybrids. The objective classification of these blizzards using a competitive neural network known as the Self-Organizing Map (SOM) demonstrates that gross segregation of the events can be achieved with a small (eight-class) map. This implies that objective analysis techniques can be used to identify these events in weather and climate model output that may aid future forecasting and risk assessment projects.

Keywords: Blizzards; blowing snow; climatology; self-organizing maps; synoptic typing

1. Introduction

The United States (US) National Weather Service (NWS) currently defines blizzards as events that have sustained winds or frequent gusts ≥ 35 mph ($16 \text{ m}\cdot\text{s}^{-1}$) and considerable falling and/or blowing snow that reduces visibilities to $\leq \frac{1}{4}$ mile (400 m) for periods of three hours or longer. These events are recorded within the National Centers for Environmental Information (NCEI) *Storm Data* publication that is reliant on submissions by the Warning Coordination Meteorologist (WCM) at each NWS forecast office. This publication serves as the official archive of storm events for the country [1,2].

Within the contiguous United States (CONUS), reported blizzards are most common over the Northern Great Plains (NGP) including the region centered on North and South Dakota [1,2]. At a county level, the highest frequencies are found along the border of North Dakota and Minnesota, which, topographically, makes up the Red River Valley (RRV) of the North (Figure 1). To some extent, this is impressive considering population-related reporting biases noted for warm-season hazardous weather events such as tornadoes [3–6]. Alternatively, reporting biases could exist by the NWS County Warning Area (CWA), as noted for warm-season hazards such as hail [7] and wind [8].

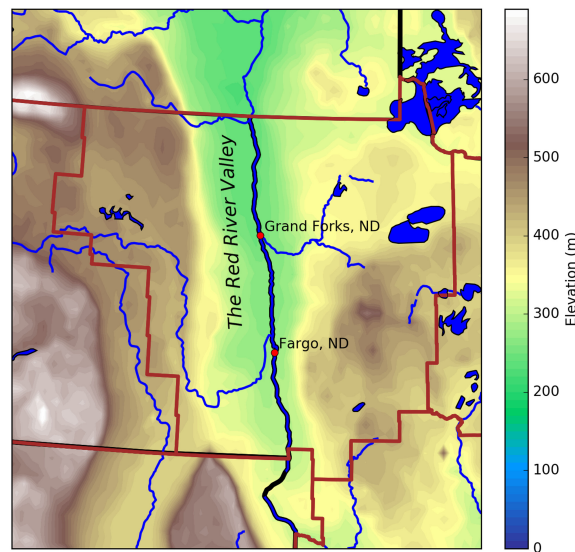


Figure 1. Topography of the Red River Valley (RRV) of the North. Elevation (ASL) is shaded while National Weather Service (NWS) County Warning Areas (CWAs) are denoted by the dark red polygons. Larger water bodies and rivers are highlighted in blue.

Regardless of potential biases in *Storm Data*, the high frequency of blizzards in this region makes physical sense and can be attributed to factors including the topography/land cover, climatology of snow cover, and frequency of high-wind events. A lake plain leftover from the receding Glacial Lake Agassiz 8000 years ago, the shallow Red River of the North flows northward to Lake Winnipeg before eventually emptying into the Hudson Bay [9]. The RRV is largely devoid of trees except within the immediate vicinity of the river and in shelterbelts (tree rows) planted due to agricultural activity. Though the RRV is, on average, only a few hundred meters deep over a 100 km width, there is evidence that winds are enhanced within this region. For example, blowing snow plumes are sometimes seen only within the RRV, typically in regimes with cold-air advection (Figure 2). While there are numerous studies that document topographic influences of valleys on winds in other locations, the authors are unaware of any existing studies for the RRV.

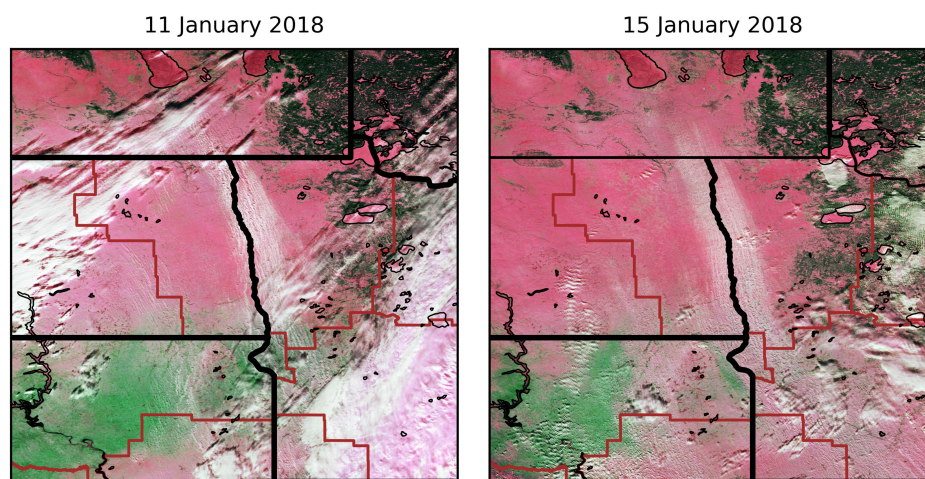


Figure 2. False color imagery (generated from I1-I2-I3-M3-M11 bands) from the Visible Infrared Imaging Radiometer Suite (VIIRS) onboard the Suomi satellite during the daylight (~1:30pm local time) overpass on (a) 11 January 2018 and (b) 15 January 2018. Snow cover is denoted by pink/red, cloud cover and blowing snow by white, and bare landscape by green (bare ground) or dark (forest) areas. Blowing snow plumes oriented along the RRV are labeled by 'BLSN'.

With a latitude of 45–49° N in the center of the North American continent, the RRV is the coldest non-mountainous region within the CONUS [10]. Though the region only receives, on average, 80–100 cm of snow in a year [11], the cold temperatures facilitate an environment that supports an average snow cover extent >85% during the winter months [12]. Snowfall events responsible for this cover have been tied to several meteorological patterns including extratropical cyclones that form due to lee cyclogenesis such as Colorado Lows and Alberta Clippers [13–17].

As the name implies, Colorado Lows originate due to cyclogenesis near its namesake (the state of Colorado). Historically, these types of systems have been associated with a number of impactful blizzards, including events such as the Children’s Blizzard on 12 January 1888 [18]. The strength of these cyclones can advect a significant amount of moisture northward, and, as a result, these systems are responsible for the heaviest (and largest scale) snowfalls in the RRV, southern Manitoba, and western Ontario [16]. The more progressive cousin of these systems include Alberta Clippers that propagate rapidly east-southeast from Canada into the upper-tier of the US [19]. Precipitation for these events typically comes in the form of mesoscale snow bands. Overall, snow totals are lower due to lack of available moisture, but these systems can still produce significant winds capable of reaching blizzard criteria [16,20]. While Colorado Lows and Alberta Clippers are colloquial terms for common North American mid-latitude cyclones, blizzards can also be forced by systems that originate in other areas (e.g., Montana). Historically, these events have been given the moniker ‘Hybrids’ by the Grand Forks NWS Forecast Office (NWSFO), and, as such, this term is used herein to describe systems that do not conform to stereotypical patterns but have a defined low pressure center. Depending on the event, snowfall can be meso- or synoptic-scale in nature, with high variability for totals.

While blizzards are often thought of as large-scale events associated with the juxtaposition of winds and snowfall associated with mid-latitude cyclones, the RRV also experiences events known as ground blizzards that are frequently driven by strong winds behind Arctic (Cold) Fronts [16,21]. For these cases, winds greater than 4–7 m·s⁻¹ impart a force on already fallen snow, rolling it on the surface before being bounced and lofted into the atmosphere [22,23]. As demonstrated in Figure 2, these events can often occur under otherwise clear skies and, in some cases, are confined solely to the RRV, providing evidence of the topographic enhancement of winds.

Historically, the Grand Forks NWSFO has subjectively classified blizzards within their CWA (see Figure 1) into the four aforementioned categories (Alberta Clippers, Arctic Fronts, Colorado Lows, and Hybrids), and has maintained a local database of these blizzards from 1974 to present. These events are identical to the reported blizzards in *Storm Data*, although additional meteorological information is sometimes included within the local dataset vs. what is officially provided in *Storm Data*. While *Storm Data* is considered the official dataset for blizzard events, the events are of such importance that the local newspaper (The Grand Forks Herald) has independently kept track of and named impactful events since the winter of 1989–1990.

The purpose of this work is two-fold. First, the climatology of blizzards within the Grand Forks NWSFO CWA will be described for the winters of 1979–1980 and 2017–2018. Besides investigating when and how often blizzards occur, this abbreviated time period will allow for composite patterns to be generated using the North American Regional Re-analysis (NARR) [24]. Given the limitations and known human biases of subjectively defining atmospheric patterns, the second goal of this work is to demonstrate that atmospheric patterns associated with these events can be objectively defined. To do so, a competitive neural network known as a Self-Organizing Map (SOM) [25] will be used.

The efforts of this work will add to the limited body of literature that discuss blizzards in continental regions such as the Northern Great Plains. The climatology and demonstration of an objective technique to classify these patterns described herein will pave the way for future studies that will seek to identify these events in re-analyses, Numerical Weather Prediction (NWP) models, and climate simulations. This will allow for questions to be investigated that range from best forecasting practices for these events to how blizzards may change in a warming climate.

2. Materials and Methods

As noted in the introduction, the climatology of blizzard events in this study comes from the publically available NCEI *Storm Data*. For the purposes of this project, only blizzards contained within the Grand Forks NWSFO CWA (Figure 1) were investigated (see Appendix A). These events are referred to as RRV blizzards due to the majority of the CWA encompassing this topographic feature, although a few counties within this region are on the periphery of the valley. To compare events to NARR data, the time period was limited to the winter seasons (October–April, determined by reported blizzards in Storm Data) of 1979–1980 and 2017–2018. Subjective classifications of event types (Alberta Clippers, Arctic Fronts, Colorado Lows, and Hybrids) were made by Grand Forks NWSFO meteorologists using available observations, model, and re-analysis output.

2.1. Composite Analysis

Composite surface and upper-air patterns were generated using the NARR [24]. Though on a native 32 km horizontal grid, this dataset was averaged to a lower resolution, 16×16 , and 1.25° (longitude) by 0.94° (latitude) grid centered on the Grand Forks NWSFO CWA. This was done to reduce the computational cost of the SOM and to facilitate future comparisons to other datasets (e.g., weather or climate model output). While a number of re-analyses are now available, NARR was chosen due to the authors' familiarity with this dataset, along with prior studies that demonstrated favorable performance over the region [25–28]. Given the variables and resolution used, it is anticipated that similar results would be found if other current generation re-analyses were used (e.g., ERA-Interim [29]). This assertion may not be valid in regions with more limited surface and upper-air observations where re-analyses are more poorly constrained.

Using storm data, available surface observations, and the NARR, midpoint times were estimated for each blizzard event. Patterns were composited for the four primary patterns using blizzard midpoint times and ± 12 -hr before and after these points. For patterns that contained a mid-latitude cyclone, the minimum mean sea level pressure (MSLP) within the domain was identified and tracked over this time.

2.2. Objective Classification Using a SOM

To objectively classify atmospheric patterns, the Self-Organizing Map (SOM) [30] technique was used. A competitive neural network, SOMs are most similar to a K-means clustering algorithm [31]. Unlike K-means clustering, SOMs include a neighborhood function during the training process. The result is a topological (feature) map that allows clusters (nodes) to a) span the data space and b) relate to each other in a two-dimensional matrix. This latter property allows users to be less concerned with the exact number of clusters to choose and instead to focus on clusters that are relevant for their analysis purposes. While this alone makes it a useful algorithm for pattern recognition, SOMs hold other advantages (handling of noise, no a priori assumptions of data, better identification of pattern mixing) over common techniques such as Principal Component Analysis (PCA)/Empirical Orthogonal Functions (EOFs) [32–34]. As a result, SOMs are now commonly used in the fields of meteorology and oceanography. For additional information, the reader is referred to earlier surveys of SOM studies [35,36].

The process of creating a SOM follows the strategy employed in earlier work by the author [37], and the reader is referred to this study for more details on the nuances of SOM creation. To summarize the process, a user must first select data for input then reduce the multi-dimensional meteorological data into input vectors that the SOM performs the clustering on. SOMs are trained in a two-step process that first determines the orientation of the feature map then iterates to a final solution that seeks to minimize the error between the training dataset and the final classification of nodes [31]. These stages require the selection of user parameters such as the map size, training length, learning rate,

and the neighborhood radius. After the SOM is created, training samples are compared to each node within the feature map and classified to the node with the minimum Euclidean distance.

Consistent with the generation of composite patterns in the previous section, the spatially averaged 16×16 , 1.25° (longitude) by 0.94° (latitude) NARR was used to train the SOM. Based on the results of the compositing process, variables that showed significant variability across patterns were used, and these included 500 hPa geopotential heights, MSLP, and surface temperatures. Other combinations of variables were tried, but the inclusion of 500 hPa geopotential heights made the largest difference in the ability of the SOM to segregate patterns. Identical to [37], variables were computed as anomalies from the field mean at each given time step. This allowed the SOM to focus on the gradients in variables, minimizing the issues of biases or variability that vary by season or exist when patterns are compared across multiple datasets (e.g., NARR vs. climate model data) which is useful for future studies. To capture the progression of systems across the domain, each training sample included time steps at the midpoint and ± 12 hrs. With three total variables, a 16×16 region, and three times for each case, input vectors used to train the SOM had a length of 2304 elements. All variables were normalized to a common scale to contribute equally to the SOMs. In total, 93 blizzard cases (a subset of 37 winters from 1979–2018 and 2015–2016) were used as input vectors due to the availability of NARR data at the time the SOM was created and as a goal to classify future patterns. Errors (Euclidean distances) for classified patterns in the latter two seasons were similar to the trained data. This suggested that (1) training the SOM with all 100 patterns would not significantly alter the results, and (2) ample variability was captured in the SOM and the methodology is useful for pattern recognition purposes.

A key parameter of the SOM (and other objective classification techniques) is the number of classes chosen. For classifications of atmospheric states, this decision will be dependent on the purpose of the study as well as the number of samples being used to train the SOM. Too few classes can smooth out the details of patterns, while too many will lead to situations where some SOM nodes have no observed patterns classified to them [37]. With a relatively small number of cases (~ 90 – 100) and the purpose of comparing the SOM to subjectively classified classes, a rectangular 8-class (4×2) is presented. Larger maps were also created, but they did not provide further insight to the results shown herein.

The SOM was generated using SOM_PAK software, which is freely available [30]. Within this package, the 'vfind' program was used; this program randomly initializes a SOM feature map a specified number of times and selects the map that minimizes the lowest quantization error. Following the guidelines of SOM_PAK [30], settings for 'vfind' included a training length that increased and learning rates and neighborhood radii that decreased between the two steps in the training process (Table 1).

Table 1. Self-Organizing Map (SOM) settings used with the SOM_PAK command 'vfind'.

Parameter	Value	Notes
Topology	Rectangular	vs. hexagonal lattice
Neighborhood Function	Bubble	vs. Gaussian
Trials	10	randomly initialized
Training Length (stage 1, stage 2)	93, 93000	# of blizzard patterns
Learning Rate (stage 1, stage 2)	0.05, 0.01	linearly decrease with time
Neighborhood Radius (stage 1, stage 2)	3, 1	# of nodes

3. Results and Discussion

3.1. General Characteristics

During the 39-year period, 100 total blizzards were reported, averaging 2.6 events per year. An annual and seasonal breakdown of these events is provided in Figure 3. RRV Blizzards are highly variable, with seasons varying from 0–10 events (Figure 3a). Record years (10 events) included the infamous 1996–1997 winter that concluded with the catastrophic RRV flood [38,39] and the 2013–2014 winter that did not have significant flooding. On the other end of the spectrum, three seasons (1986–1987, 1990–1991, and 2011–2012) did not have any recorded blizzards. While the source of this

variability is beyond the scope of this study, snowfall and cyclone variability in this region have been tied in part to phases of the El Niño Southern Oscillation (ENSO) and the North American Oscillation (NAO) [40,41].

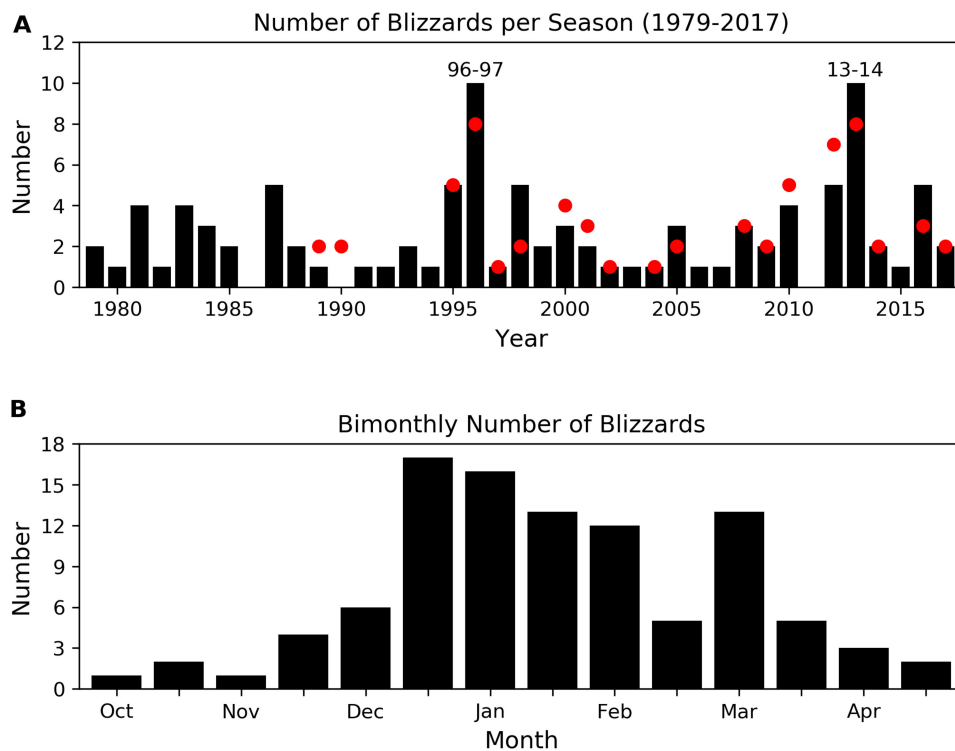


Figure 3. (a) Annual and (b) bimonthly number of *Storm Data* blizzards for the winter seasons of 1979–1980 and 2017–2018. Named blizzards by the Grand Forks Herald are provided by the red dots in panel (a).

Out of curiosity, named blizzards from the Grand Forks Herald newspaper were also compared for annual totals. Over the shorter period (1989–1990 and 2017–2018), the newspaper named 63 (vs. 76) blizzards, and the datasets had a correlation of 0.77. Provided that the distribution area for the paper is smaller than the CWA, these results are expected. While some specific years had more events recorded by the paper vs. *Storm Data*, this is attributed to events that were stronger winter storms but did not meet official blizzard criteria.

Blizzards have been reported from October–April, with the bulk of the events occurring from the 2nd half of December to the 1st half of March (Figure 3b). The most frequent period of occurrence was the 2nd half of December, with a total of 17 blizzards over the 39-year period. A unique aspect of the seasonal cycle is the bimodal distribution with a well-defined lull in late February. This is in agreement with North American cyclone climatologies that indicate a relative minima of cyclones during February [42].

3.2. Composite Analysis

Classifications of the 100 classified blizzards were used to generate composite patterns from the NARR. Of the 100 patterns, two patterns were sufficiently different that they did not fit any of the four categories, and these were omitted from the composite analysis. These included two events driven by southerly winds well ahead of weaker mid-latitude cyclones on 6 March 2014 and 31 December 1996. The remaining composite patterns are now described.

Of the four patterns, Colorado Low blizzards feature the strongest mid-latitude cyclone (Figures 4a–7a) and resemble prior composites of this type [43]. Tracking from Northeast Colorado to North Wisconsin, the composite minimum MSLP decreases from 1002–1000 hPa from 12 h prior to

the midpoint of the event. With a storm track south of the RRV, the region is predominately under northerly surface winds that strengthen and shift direction from the East-Northeast to the Northwest as the cyclone progresses eastward. While not shown (and noted earlier), these systems are responsible for the highest snowfall totals, as the region falls within the precipitation shield north of the cyclone track [44]. Aloft, these events are associated with the progression of a well-defined trough that deepens over the region (Figures 5 and 7a). In response to the passage of this trough, strong 500 hPa height falls are found leading up to the event, with the maximum decrease located just northeast of the surface low. In some cases, these troughs are associated with an upper-level closed low, although this definition has been lost to some extent during the compositing process.

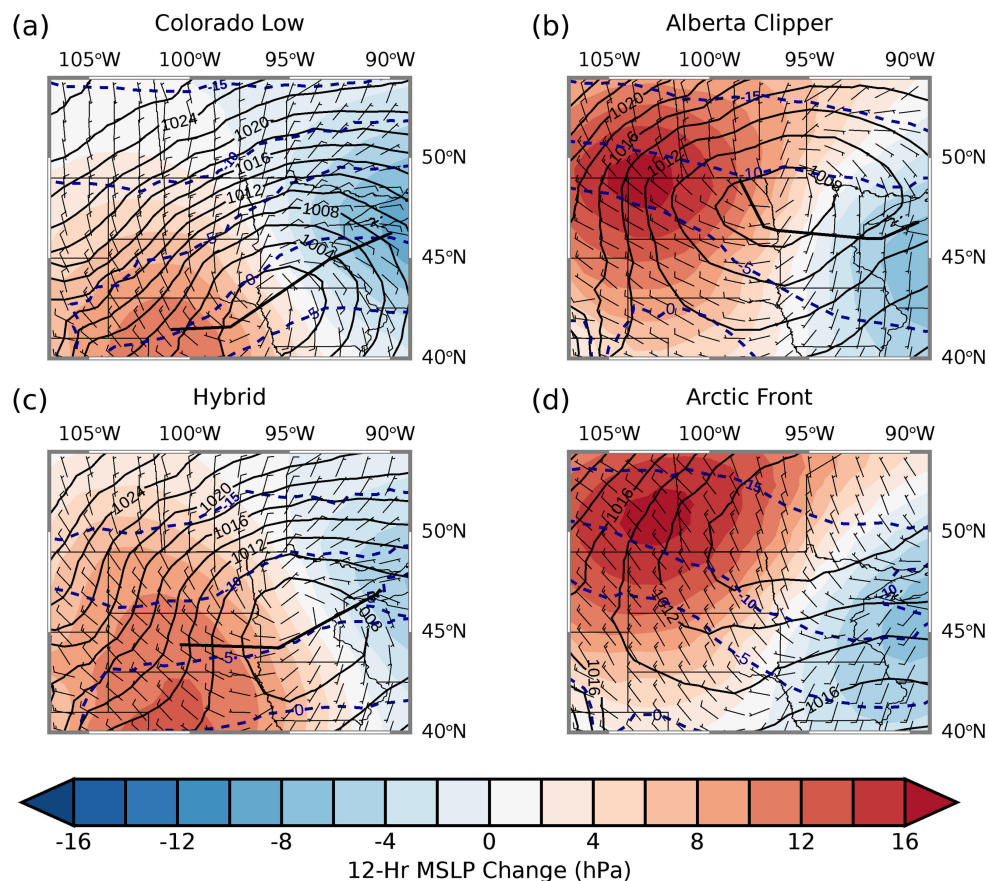


Figure 4. North American Regional Re-analysis (NARR) composite plots of mean sea level pressure (MSLP) (hPa), surface wind barbs (kts), and surface temperatures ($^{\circ}\text{C}$) 12 hr prior to the midpoint of (a) Colorado Low, (b) Alberta Clipper, (c) Hybrid, and (d) Arctic Front blizzards. 12-h MSLP change (midpoint—12 hr prior) is provided by shaded contours while composite mean cyclone tracks are denoted by the thick black lines for select classes.

Blizzards associated with Alberta Clippers also feature a well-defined, albeit weaker (1008–1006 hPa) mid-latitude cyclone (Figures 4b–7b). Consistent with the name and prior composites [19], these systems track east-southeast from southern Canada across the RRV with the cyclone center eventually reaching Northeast Minnesota and North Wisconsin. One should note that the composite cyclone tracks appear to be shifted east compared to the Colorado Low and barely encompass the passage of the low out of Canada. Because these tracks were identified symmetrically around the midpoint of the blizzard conditions, this implies that poor visibility primarily occurs after the passage and development of the surface cyclone (Figure 4b). Aloft, conditions leading up to the event feature stronger west-northwest 500 hPa flow with maximum height falls located over Minnesota, just ahead of a developing short-wave trough (Figure 5b). By the midpoint of the blizzard,

this trough has amplified and progressed eastward across the domain with 500 hPa winds shifting to the Northwest.

As noted earlier, the Grand Forks NWS defines Hybrid events as those with characteristics of multiple patterns, and this is also true of the composite patterns (Figures 4c–7c). At the surface, this class manifests itself as a mid-latitude cyclone track that begins farther north (south) of a Colorado Low (Alberta Clipper). The minimum pressure and intensity of the wind field are similar to that of the Alberta Clipper, but it has weaker 12-hr pressure rises/falls (Figure 6c). This latter property can be attributed to the slower progression of Hybrids vs. Alberta Clippers. At 500 hPa, Hybrids are associated with weaker, near-zonal flow 12 h prior to the midpoint of blizzard conditions (Figure 4c). Compared to the Alberta Clippers, the short-wave trough is in a similar position, but the orientation of the flow leads to a more neutral tilt. Unlike the aforementioned pattern, Hybrids feature more deepening of the upper-level low/trough by the midpoint of the blizzard, similar to what is seen for Colorado Lows.

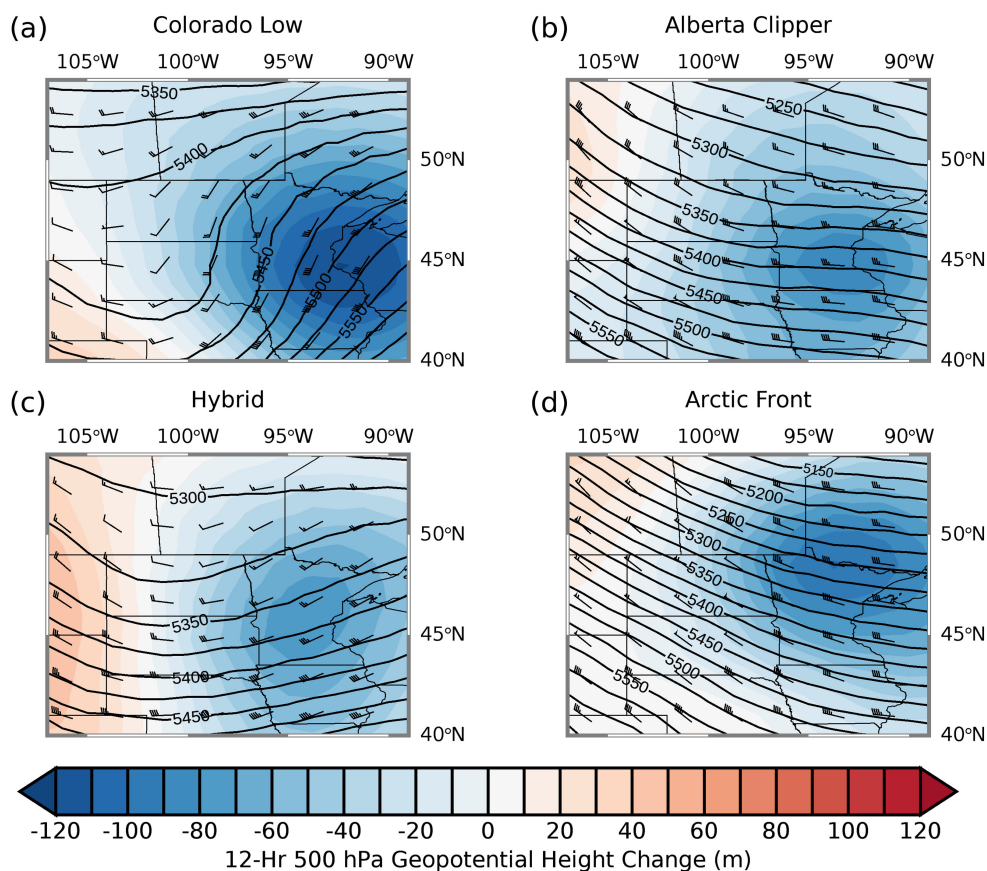


Figure 5. NARR composite plots of 500 hPa Geopotential heights (m) and wind barbs (kts) 12 hr prior to the midpoint of (a) Colorado Low, (b) Alberta Clipper, (c) Hybrid, and (d) Arctic Front blizzards. 12-h 500 hPa height change (midpoint—12 hr prior) is provided by shaded contours.

Arctic Fronts are the final, and arguably most unique, composite pattern identified with RRV blizzards (Figures 4d–7d). Unlike the other patterns, no centralized region of low-pressure is seen at the surface. Instead, this pattern features an elongated southwest to northeast oriented surface trough associated with the developing Arctic Front (Figure 4d). As the event progresses, surface pressures rapidly rise and northerly winds strengthen behind the front, as the Arctic High develops to the Northwest, increasing the gradient in MSLP and Cold Air Advection (CAA). Because the surface trough/Arctic Front is often associated with a more distant cyclone, 500 hPa patterns are more dissimilar from the other patterns (Figures 5 and 7d). These events are characterized by strong northwest flow

that eventually develops a southwest trough (passing vorticity maxima) in the eastern half of the domain by the mid-point of the event. As a result, the region ends up residing under large (60 m) height rises associated with a strengthening jet stream and implied Negative Vorticity Advection (NVA). Compared to the Alberta Clippers and Hybrid events, 500 hPa winds associated with Arctic Fronts are approximately double in magnitude (80 vs. 40 kts). This leads to a vertical wind profile (not shown) that implies downward transfer of momentum in a regime of subsidence is a key mechanism for reaching blizzard criteria for winds. The presence of CAA, NVA, and subsidence matches many of the checklist items for impactful post-cold frontal winds [21].

Meteorological patterns responsible for blizzard events have preferred periods of occurrence (Figure 8). Early and late season events (October, November, and April) are primarily due to Hybrid and Colorado Lows, with only one (Alberta Clipper) event not fitting these categories. These classes have bimodal distributions with Colorado Lows (Hybrids) peaking in December and March (January and March), respectively. Alberta Clippers occur from December to March, with the majority of the events occurring during January and February, consistent with [19]. Arctic Fronts, commonly responsible for ground blizzards, are more common during the late winter with events between December to March and a maximum in January. As a result of these distributions, January ends up being the most diverse month with relatively constant fractions (0.2–0.3) across the categories (Figure 8b). As noted earlier, the lull in February is consistent with extra-tropical cyclone climatologies, and this is seen in Figure 8 as a reduction of Colorado and Hybrid lows in this month.

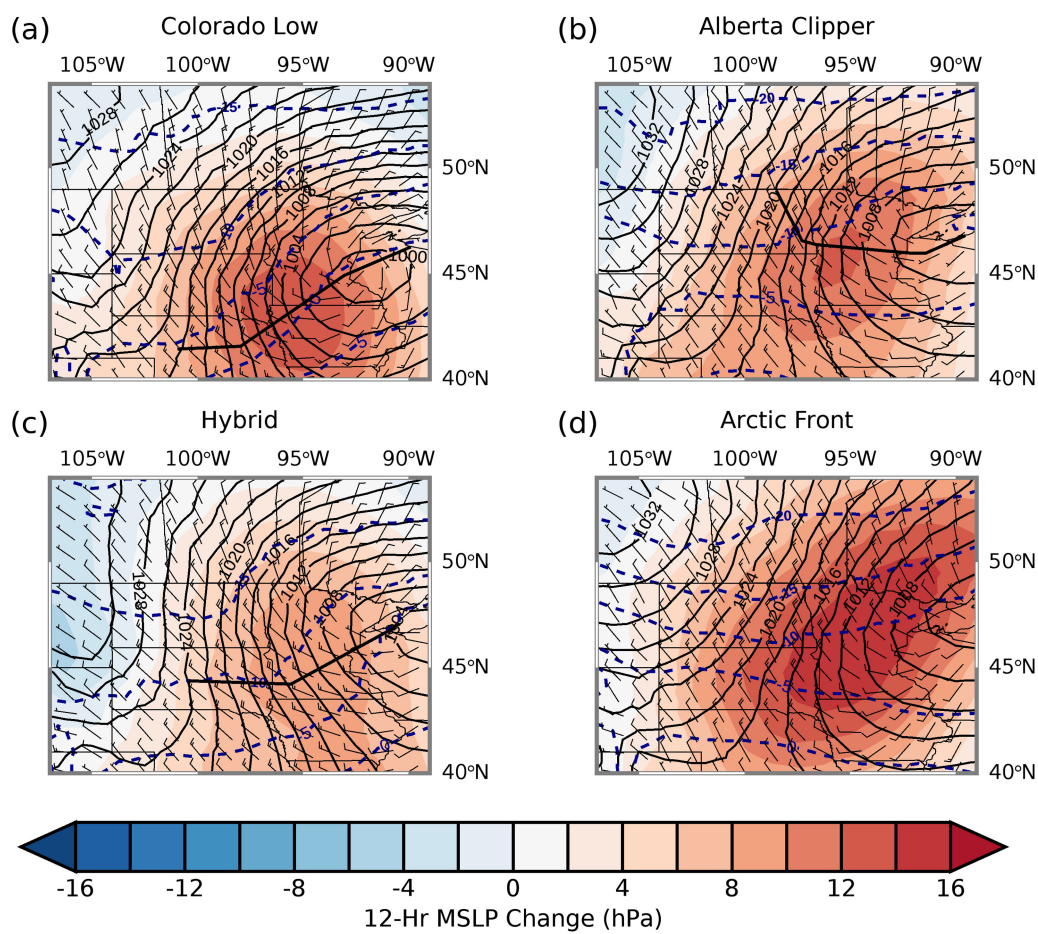


Figure 6. As in Figure 4, except for the midpoint of the blizzard. 12 hr MSLP change (12 hr post—midpoint) is provided by shaded contours.

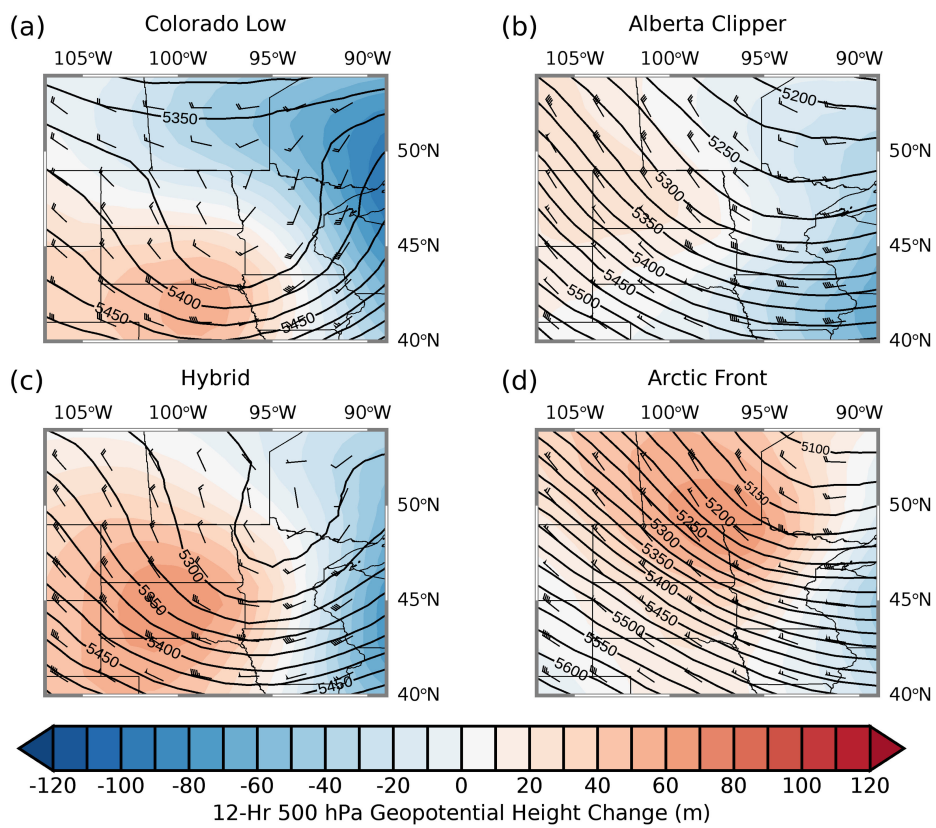


Figure 7. As in Figure 5, except for the midpoint of the blizzard. 12-h 500 hPa height change (12 hr post—midpoint) is provided by shaded contours.

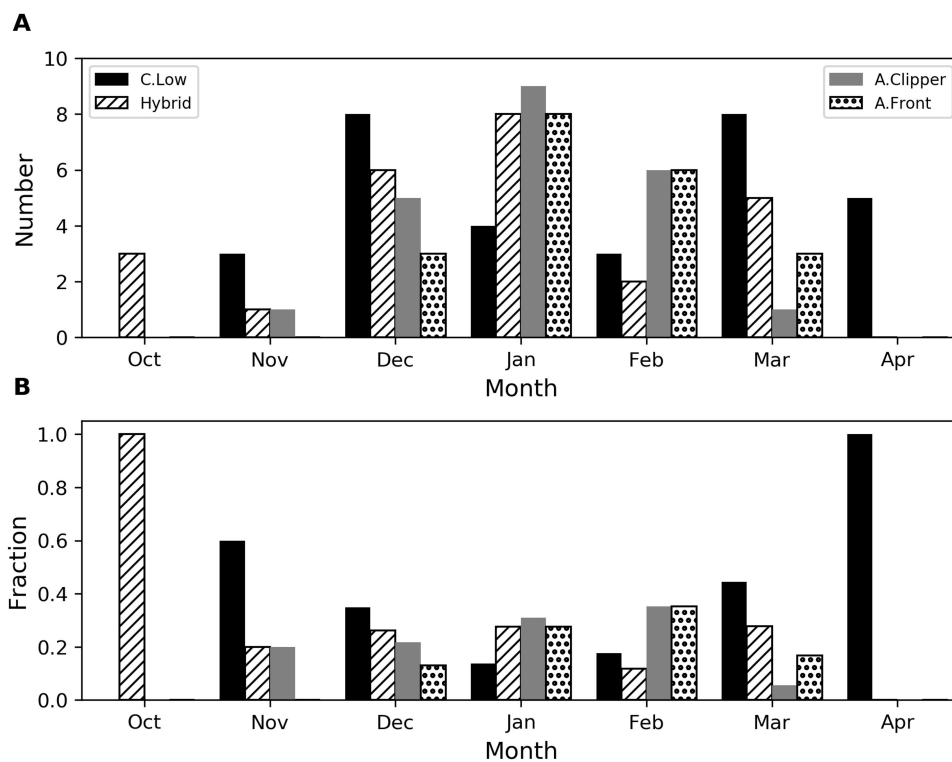


Figure 8. (a) Number and (b) fraction of monthly blizzards for the winter seasons of 1979–1980 and 2017–2018, separated by type.

3.3. Objective Classification of Patterns Using a SOM

Surface and 500 hPa analyses for the midpoint of blizzard events in the eight-class SOM are shown in Figures 9 and 10. The SOM shows a progression of patterns that shift from cold fronts associated with CAA (nodes 1/5) to deeper surface lows (nodes 3/4/7/8). These patterns have 500 hPa analyses similar to those seen in earlier composites. For example, nodes 1/5 resemble Arctic Front patterns with a strong northwesterly flow aloft, while the rightmost nodes appear as Colorado Lows with either upper-level toughing (nodes 3/4) or a closed low (node 7/8). The progression of systems is also similar to the composites shown earlier (not shown). For example, the rightmost nodes (4/8) progress northeastward like a Colorado Low. Shifting from right-to-left, the mid-latitude cyclones become weaker and have tracks that are displaced northerly, consistent with Hybrid/Alberta Clipper type systems. While the SOM has many positive traits when compared to the composites, it by no means is a perfect reproduction of the subjectively classified classes. For example, Arctic Fronts have pressures that are too low 12-hrs prior to the midpoint of events resulting in weak cyclones vs. the open trough seen in Figure 4. This is undoubtedly a result of the neighborhood function within the SOM smoothing this category with other mid-latitude cyclone nodes. Despite this issue, quantitative comparisons of blizzards events to both the composite patterns, and the eight-class SOM yielded better agreement for the SOM with mean Euclidean distance $\sim 30\%$ lower (315.6 vs. 444.1). Increasing the SOM to a 5×3 (or larger) map mitigates this issue and further lowers the mean Euclidean distance; however, this happens at the expense of decreasing the number of blizzards that occur per class (not shown).

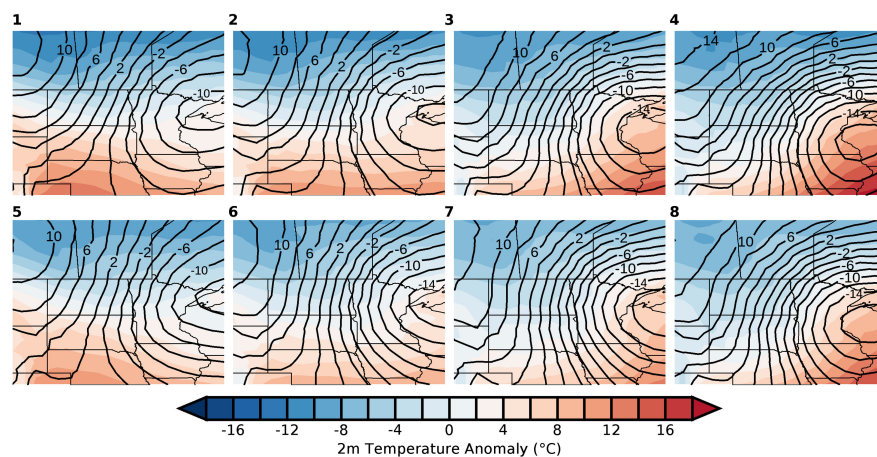


Figure 9. MSLP (hPa, dashed lines) and surface temperature (°C, filled contours) anomalies during the midpoint of blizzards for the eight-class (2×4) SOM. Nodes are identified by the external numbers ranging from 1–4 (5–8) for the top (bottom) rows.

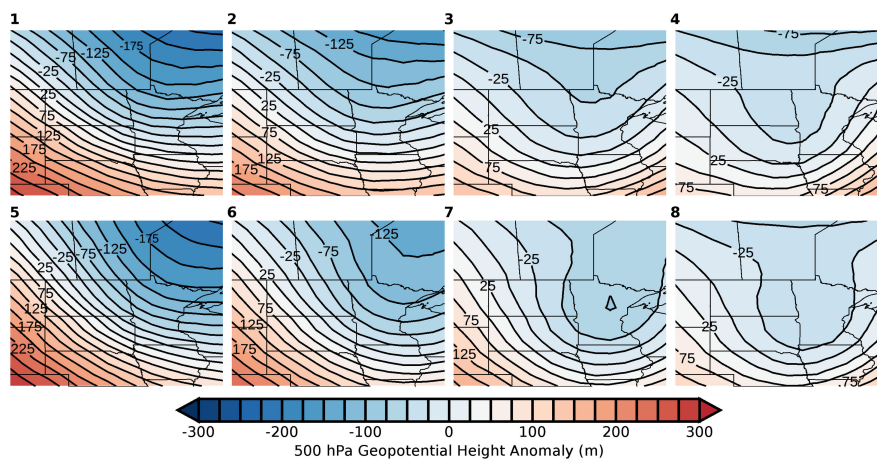


Figure 10. As in Figure 9, except for 500 hPa height anomalies (shaded and dashed contours).

As a final test of the SOM’s ability to segregate patterns, the subjectively classified events were categorized into the eight-class SOM (Figure 11). As expected by the meteorological interpretation of the nodes, patterns have distinct areas of occurrence. Colorado Lows (Figure 11a) only occur on the right-hand-side of the SOM, with the majority of the cases occurring within Node 4. Alberta Clippers occur within the left-most six nodes, with most occurring within Nodes 1, 2, 6, and 7. Hybrids, which are subjectively defined as patterns with features of multiple patterns are the only category to occur within every node. That said, the majority of these cases occur within Nodes 3 and 7, in-between Colorado Lows and Alberta Clippers. Finally, Arctic Fronts are primarily on the left-hand-side of the SOM with the majority of the cases occurring in Node 5. From a probability stand-point, categories within the SOM can be arranged in a column fashion, with probability of occurrence shifting from Arctic Fronts (Nodes 1/5), to Alberta Clippers (Nodes 2/6), to Hybrids (Nodes 3/7), to Colorado Lows (Nodes 4/8). By doing this, the time period of occurrence for these categories gives results similar to the results shown in Figure 8 with seasonal occurrence of SOM nodes varying by column (Table 2).

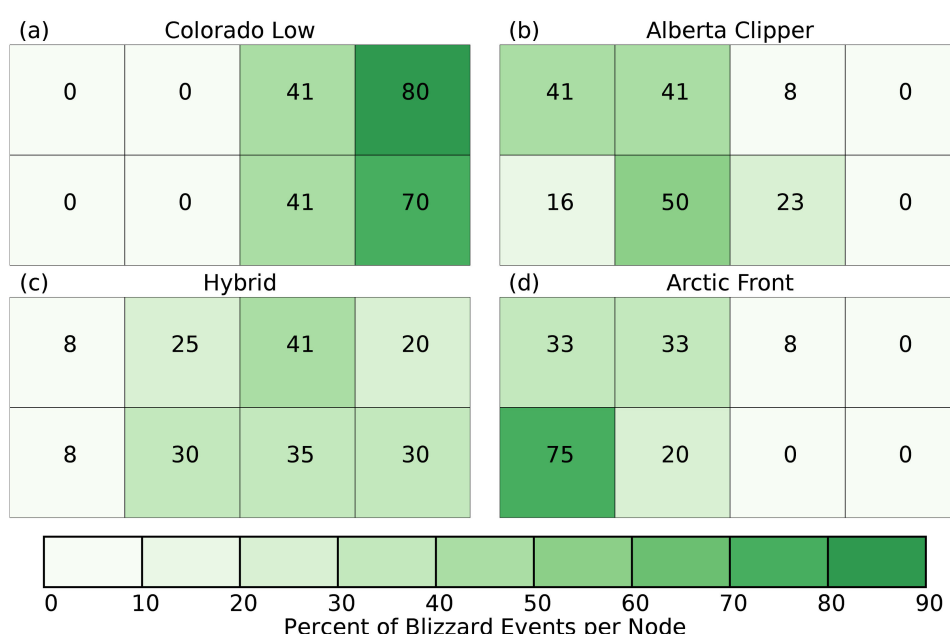


Figure 11. Percent of (a) Colorado Low, (b) Alberta Clipper, (c) Hybrid, and (d) Arctic Front blizzards identified within each of the eight SOM nodes.

Table 2. Number (Percentage) of blizzards segregated by month and SOM nodes. Percentages are calculated using monthly totals.

	Nodes 1/5 (Arctic Front)	Nodes 2/6 (Alberta Clipper)	Nodes 3/7 (Hybrid)	Nodes 4/8 (Colorado Low)
October	0 (0)	0 (0)	2 (67)	1 (33)
November	0 (0)	0 (0)	2 (40)	3 (60)
December	2 (9)	7 (30)	9 (39)	5 (22)
January	12 (41)	5 (17)	8 (28)	4 (14)
February	6 (35)	6 (35)	3 (18)	2 (12)
March	4 (22)	4 (22)	4 (22)	6 (33)
April	0 (0)	0 (0)	1 (20)	4 (80)

3.4. Discussion and Future Work

The good agreement between subjectively and objectively identified blizzard patterns provides evidence that the characteristics of these events, including types of patterns and time periods of occurrence, are well understood. The use of a relatively small SOM and inclusion of only several

variables to obtain this finding is a positive result that suggests SOMs can be used to investigate a number of outstanding questions regarding blizzards. Some of these activities are now discussed.

Within the realm of weather prediction, a constant struggle is determining whether visibility criteria will be met to justify and verify products such as NWS blizzard warnings. Though blowing snow parametrizations exist [45,46], they are not currently included in operational Numerical NWP models within the US. Instead, local forecasters must use empirical models that determine a probability of blowing snow given conditions such as wind speed, air temperature, and snowpack conditions [47]. The context of how these events fit within the scope of forcing mechanism (type of event) is currently only considered subjectively (e.g., Arctic Fronts are harder to forecast than Colorado Lows). A possible solution is for SOMs to provide real-time identification and classification of forecast atmospheric patterns from deterministic or ensemble NWP systems. While this could be done subjectively, burden is placed on the forecaster to identify patterns within the large range of modeling systems now available. Further, there is always the issue of human bias. A hypothetical system can identify the fractional number of ensemble members with forecasted blizzard patterns. Pattern typing can then inform forecasters on the scope of impacts. For a system such as the Global Ensemble Forecast System (GEFS), doing this subjectively would require the forecaster to individually inspect 21 members, a process that is too arduous for an operational setting.

Prior to the implementation of such a system, the SOM must consider null cases to understand the nuances between patterns that do and do not produce blizzard conditions. In practice, this can be done in two different ways. As presented here, a small SOM developed solely from blizzard events can be used by defining a threshold Euclidean distance that counts a pattern as a hit. A caveat with the presented SOM is distances that are still quite large; this would lead to a higher risk of false alarms. Instead, a larger SOM could be used to reduce the threshold Euclidean distance needed. Alternatively, SOMs can be produced using all available patterns during the winter. To encompass the increased variability in patterns (blizzard and null cases alike), these SOMs must be larger. Instead of using a threshold to define events, observed blizzard events can be mapped to the larger SOM to understand which nodes are associated with these events.

Regardless of the exact methods, an interesting avenue of future work is a retrospective analysis on all historical patterns. This can provide insight into events that may have been missed by the observation system or were too limited in scope to fit within the traditional zone/county verification process at the NWS. Pattern recognition can also be extended farther back in time using datasets such as the 20th Century Re-analysis [48] to yield a long-term climatology of blizzards.

How the frequency and intensity of RRV blizzards may change in a warming climate is also unknown. Previous studies have focused on how precipitation or cyclone frequency may change independently. From the Clausius–Clapeyron relationship, a warmer climate will dictate higher amounts of column water vapor and, thus, precipitation [49]. During the winter, however, there will be a balance between warmer temperatures, column water vapor, and precipitation phase. Overall, a general decline in snow cover has been found for the northern hemisphere, and much of this is due to a significant shortening of the snowy season [50,51]. Despite this trend, the RRV region has seen an increase in snowfall, especially for higher end events with 2+ inches [52,53].

Regarding forcing mechanisms for RRV blizzards, mixed results have been found for extratropical cyclones. While some studies suggest a decrease in Northern Hemisphere wintertime cyclone frequency [54,55], other work suggests the strongest cyclones have intensified or could further intensify in future climate projections [56–59]. Concerning specific patterns identified within the present study, there is a projected decrease (increase) in Alberta Clippers (Colorado Lows) over North America [59]. It is unknown how Hybrid lows or Arctic Fronts may change, and this is an avenue of work into which SOMs can provide insight, as they can provide information on type and frequency of occurrence of patterns.

4. Summary

A climatology of documented blizzard events within Storm Data for the Grand Forks NWSFO CWA for the winter seasons of 1979–1980 and 2017–2018 was presented. The NARR was used to composite and objectively classify patterns. These results are now summarized.

- Over the past 39 years, 100 documented blizzards were reported in *Storm Data*, resulting in an average of 2.6 blizzards per year. This dataset strongly correlates with an unofficial record of societally impactful events named by the Grand Forks Herald, a local newspaper.
- RRV blizzards occur between October and April and have a distinct bimodal distribution of occurrence, with 58% of the events occurring from December 15th to February 15th. After a lull in late February, a separate (weaker) maxima occurs in March.
- The Grand Forks NWSFO has subjectively classified blizzard patterns into four classes: Alberta Clippers, Arctic Fronts, Colorado Lows, and Hybrids. Composite patterns resemble the expected meteorological patterns with variations in the intensity, position, and progressiveness of the mid-latitude cyclone and upper-level trough. Hybrids appear as lows that have tracks in-between the Alberta Clipper and Colorado Low systems.
- Patterns have seasonal variability, with most early/late season blizzards caused by Colorado and Hybrid Lows. Alberta Clippers and Arctic Fronts are more common in the middle of the winter with peak occurrence of these latter patterns in January–February.
- A relatively simple eight-class (4×2) SOM can reproduce the general characteristics of the composite patterns. A transition in patterns is seen from Colorado Lows → Hybrids → Alberta Clippers → Arctic Fronts. This results in reasonable separation of subjectively identified events and good agreement in the seasonality of these patterns. This adds confidence to the subjective classification of patterns.

While these results are most relevant to the local populace, the last point has important ramifications for the broader weather and climate communities. Impactful weather events such as blizzards are challenging to forecast/detect over both short and long time-scales due to properties (e.g., visibility) that are not explicitly simulated by weather and climate models. The success of the SOM technique to objectively classify patterns suggests that pattern recognition can be used to address problems such as the predictability of hazardous weather events in NWP ensembles or trends in these events in climate simulations. These subjects are the topics of forthcoming work.

Author Contributions: Conceptualization, A.K. and A.T.; Formal analysis, A.T.; Funding acquisition, A.K.; Investigation, A.T.; Methodology, A.K.; Project administration, A.K.; Supervision, T.G. and G.G.; Visualization, A.T.; Writing—original draft, A.K.; Writing—review and editing, A.K., T.G. and G.G.

Funding: This research was funded by the National Science Foundation Project IIA-1355466 at the University of North Dakota.

Acknowledgments: This paper is dedicated to the late Dave Kellenbenz, a general forecaster at the Grand Forks NWSFO who passed away in 2016 after a courageous battle with Melanoma. Dave maintained the database of blizzards at this office and provided this dataset to the authors prior to his passing that motivated much of this work. The list of named blizzards from the Grand Forks Herald was provided by reporter Tess Williams. NARR data was provided by the NOAA/OAR/ESRL PSD, Boulder, Colorado, USA, from their Web site at <http://www.esrl.noaa.gov/psd/>.

Conflicts of Interest: The authors declare no conflict of interest.

Appendix A

Table A1. Storm Data Blizzards in the Grand Forks NWSFO CWA 1979–1980 and 2017–2018. Italicized events were not included in the typing or SOM analyses. Blizzards named by the Grand Forks Herald but not listed within *Storm Data* are not provided. These events were most likely winter storms with visibility, wind speed, or duration not meeting NWS thresholds.

Year	Month	Day	Midpoint Hour in NARR (UTC)	Type	Grand Forks Herald Name (1989–2018)
2018	1	11	0	Front	Betsy
2017	12	4	21	Colorado	Axl
2017	3	7	6	Hybrid	
2017	1	12	18	Front	Carrie
2016	12	26	15	Colorado	Blitzen
2016	12	7	12	Hybrid	Alvin
2016	11	18	12	Colorado	
2016	2	8	9	Clipper	
2015	1	8	21	Clipper	Beryl
2015	1	3	12	Clipper	Andrew
2014	3	31	21	Colorado	Gigi
2014	3	21	15	Front	
2014	3	6	0	Ground	
2014	2	26	21	Front	
2014	2	13	12	Clipper	Fred
2014	1	26	18	Clipper	Era Bell
2014	1	22	12	Front	Dillon
2014	1	16	12	Front	Corene
2014	1	4	6	Clipper	Bubba
2013	12	28	21	Front	Anita
2013	3	18	9	Hybrid	Fiona
2013	2	18	21	Hybrid	Dolley
2013	2	11	3	Colorado	Cooper
2013	1	19	18	Front	Beth
2013	1	12	3	Colorado	Aaron
2011	3	12	6	Clipper	Estra
2011	1	1	9	Colorado	Dave
2010	12	30	21	Colorado	Casey
2010	10	27	9	Hybrid	Adeline
2010	1	25	18	Clipper	Brett
2009	12	26	3	Colorado	Alvin
2009	3	10	21	Colorado	Coyote
2009	1	12	15	Clipper	Barack
2008	12	14	15	Colorado	
2008	2	9	18	Front	
2007	3	3	0	Hybrid	
2006	1	24	15	Front	
2005	11	16	3	Clipper	York
2005	10	6	3	Hybrid	Zach
2005	1	22	6	Clipper	Ann
2004	2	11	18	Clipper	
2003	2	11	18	Front	Arlys
2001	12	23	0	Colorado	Bonnie
2001	10	25	0	Hybrid	Al
2001	2	25	12	Colorado	Dale
2000	12	21	3	Clipper	Carol
2000	12	16	15	Hybrid	Bill
2000	3	9	3	Colorado	
1999	12	19	18	Clipper	
1999	4	1	18	Colorado	
1999	3	17	18	Hybrid	
1999	2	12	12	Front	
1998	12	18	21	Clipper	

Table A1. Cont.

Year	Month	Day	Midpoint Hour in NARR (UTC)	Type	Grand Forks Herald Name (1989–2018)
1998	11	10	21	Colorado	Alex
1998	3	13	18	Front	Aurora
1997	4	6	12	Colorado	Hannah
1997	3	4	9	Colorado	Gust
1997	1	22	12	Hybrid	Franzi
1997	1	15	21	Front	Elmo
1997	1	10	9	Clipper	Doris
1997	1	5	9	Colorado	
1996	12	31	21	Valley	
1996	12	21	12	Front	Christopher
1996	12	18	0	Clipper	Betty
1996	11	17	9	Colorado	Andy
1996	3	25	0	Colorado	Erin
1996	2	27	21	Hybrid	Darrel
1996	2	10	21	Clipper	
1996	1	18	12	Hybrid	Bruno
1995	12	9	0	Hybrid	Anna
1995	2	10	6	Clipper	
1994	4	26	15	Colorado	
1993	12	22	0	Clipper	
1992	12	25	6	Front	
1991	12	14	3	Hybrid	Dagmar
1990	1	11	12	Clipper	Arnie
1989	2	1	6	Front	
1989	1	7	21	Hybrid	
1988	3	12	3	Colorado	
1988	2	14	15	Clipper	
1988	1	24	21	Hybrid	
1988	1	12	15	Hybrid	
1987	12	31	3	Colorado	
1986	4	15	3	Colorado	
1985	11	19	3	Hybrid	
1985	3	4	6	Colorado	
1985	1	25	0	Front	
1984	12	16	18	Colorado	
1984	3	10	15	Front	
1984	2	5	6	Front	
1983	12	25	0	Hybrid	
1983	12	15	9	Hybrid	
1983	3	8	21	Colorado	
1982	4	3	12	Colorado	
1982	3	8	15	Hybrid	
1982	1	23	15	Colorado	
1982	1	10	18	Hybrid	
1981	2	1	12	Colorado	
1980	1	11	15	Hybrid	
1980	1	7	3	Hybrid	

References

1. Schwartz, R.M.; Schmidlin, T.W. Climatology of Blizzards in the Conterminous United States, 1959–2000. *J. Clim.* **2002**, *15*, 1765–1772. [[CrossRef](#)]
2. Coleman, J.S.; Schwartz, R.M. An Updated Blizzard Climatology of the Contiguous United States (1959–2014): An Examination of Spatiotemporal Trends. *J. Appl. Meteorol. Climatol.* **2017**, *56*, 173–187. [[CrossRef](#)]
3. Doswell, C.A.; Moller, A.R.; Brooks, H.E. Storm spotting and public awareness since the first tornado forecasts of 1948. *Weather Forecast.* **1999**, *14*, 544–557. [[CrossRef](#)]
4. Ray, P.S.; Bieringer, P.; Niu, X.; Whissel, B. An improved estimate of tornado occurrence in the central plains of the United States. *Mon. Weather Rev.* **2003**, *131*, 1026–1031. [[CrossRef](#)]

5. Anderson, C.J.; Wikle, C.K.; Zhou, Q. Population influences on tornado reports in the United States. *Weather Forecast.* **2007**, *22*, 571–579. [[CrossRef](#)]
6. Elsner, J.B.; Michaels, L.E.; Scheitlin, K.N.; Elsner, I.J. The Decreasing Population Bias in Tornado Reports across the Central Plains. *Weather Clim. Soc.* **2013**, *5*, 221–232. [[CrossRef](#)]
7. Allen, J.T.; Tippett, M.K. The characteristics of United States hail reports: 1955–2014. *Electron. J. Sev. Storms Meteorol.* **2015**, *10*, 1–31.
8. Weiss, S.J.; Hart, J.A.; Janish, P.R. An examination of severe thunderstorm wind report climatology: 1970–1999. In Proceedings of the 21st Conference Severe Local Storms, San Antonio, TX, USA, 11–16 August 2002; pp. 446–449.
9. Teller, J.T. Proglacial lakes and the southern margin of the Laurentide Ice Sheet. In *North America and Adjacent Oceans during the Last Deglaciation*; Ruddiman, W.F., Wright, H.E., Jr., Eds.; Geological Society of America: Boulder, CO, USA, 1987; pp. 39–69.
10. Climate Data Online (CDO). Available online: <https://www.ncdc.noaa.gov/cdo-web/> (accessed on 10 December 2018).
11. Kluver, D.; Mote, T.; Leathers, D.; Henderson, G.R.; Chan, W.; Robinson, D.A. Creation and Validation of a Comprehensive 1° by 1° Daily Gridded North American Dataset for 1900–2009: Snowfall. *J. Atmos. Ocean. Technol.* **2016**, *33*, 857–871. [[CrossRef](#)]
12. Estilow, T.W.; Young, A.H.; Robinson, D.A. A long-term Northern Hemisphere snow cover extent data record for climate studies and monitoring. *Earth Syst. Sci. Data* **2015**, *7*, 137–142. [[CrossRef](#)]
13. Newton, C.W. Mechanisms of circulation change in a lee cyclogenesis. *J. Meteorol.* **1956**, *13*, 528–539. [[CrossRef](#)]
14. Reitan, C.H. Frequencies of cyclones and cyclogenesis for North America, 1951–1970. *Mon. Weather Rev.* **1974**, *102*, 861–868. [[CrossRef](#)]
15. Zishka, K.M.; Smith, P.J. The climatology of cyclones and anticyclones over North America and surrounding ocean environs for January and July, 1950–77. *Mon. Weather Rev.* **1980**, *108*, 387–401. [[CrossRef](#)]
16. Stewart, R.E.; Bachand, D.; Dunkley, R.R.; Giles, A.C.; Lawson, B.; Legal, L.; Miller, S.T.; Murphy, B.P.; Parker, M.N.; Paruk, B.J.; et al. Winter storms over Canada. *Atmos.-Ocean* **1995**, *33*, 223–247. [[CrossRef](#)]
17. Hoskins, B.J.; Hodges, K.I. New perspectives on the Northern Hemisphere winter storm tracks. *J. Atmos. Sci.* **2002**, *59*, 1041–1061. [[CrossRef](#)]
18. Laskin, D. *The Children's Blizzard*, 3rd ed.; HarperCollins: New York, NY, USA, 2005; p. 336.
19. Thomas, B.C.; Martin, J.E. A Synoptic Climatology and Composite Analysis of the Alberta Clipper. *Weather Forecast.* **2007**, *22*, 315–333. [[CrossRef](#)]
20. Schultz, D.M.; Doswell, C.A. Analyzing and Forecasting Rocky Mountain Lee Cyclogenesis Often Associated with Strong Winds. *Weather Forecast.* **2000**, *15*, 152–173. [[CrossRef](#)]
21. Kapela, A.F.; Leftwich, P.W.; Van Ess, R. Forecasting the impacts of strong wintertime post-cold front winds in the northern plains. *Weather Forecast.* **1995**, *10*, 229–244. [[CrossRef](#)]
22. Mellor, M. *Blowing Snow*; US CRREL Monogr: Hanover, NH, USA, 1965; p. 79.
23. Li, L.; Pomeroy, J.W. Probability of occurrence of blowing snow. *J. Geophys. Res.* **1997**, *102*, 21955–21964. [[CrossRef](#)]
24. Mesinger, F.; DiMego, G.; Kalnay, E.; Mitchell, K.; Shafran, P.C.; Ebisuzaki, W.; Jović, D.; Woollen, J.; Rogers, E.; Berbery, E.H.; et al. North American regional reanalysis. *Bull. Am. Meteorol. Soc.* **2006**, *87*, 343–360. [[CrossRef](#)]
25. Pielke, R., Sr.; Nielsen-Gammon, J.; Davey, C.; Angel, J.; Bliss, O.; Doesken, N.; Cai, M.; Fall, S.; Niyogi, D.; Gallo, K.; et al. Documentation of uncertainties and biases associated with surface temperature measurement sites and for climate change assessment. *Bull. Am. Meteorol. Soc.* **2007**, *88*, 913–928. [[CrossRef](#)]
26. Choi, W.; Kim, S.J.; Rasmussen, P.F.; Moore, A.R. Use of the North American Regional Reanalysis for hydrological modelling in Manitoba. *Can. Water Resour. J.* **2009**, *34*, 17–36. [[CrossRef](#)]
27. Kim, S.J. Evaluation of surface climate data from the North American Regional Reanalysis for Hydrological Applications in Central Canada. Ph.D. Thesis, University of Manitoba, Winnipeg, Canada, 2012.
28. King, A.T.; Kennedy, A.D. North American Supercell Environments in Atmospheric Reanalyses and RUC-2. *J. Appl. Meteorol. Climatol.* **2019**, *58*, 71–92. [[CrossRef](#)]

29. Dee, D.P.; Uppala, S.M.; Simmons, A.J.; Berrisford, P.; Poli, P.; Kobayashi, S.; Andrae, U.; Balmaseda, M.A.; Balsamo, G.; Bauer, P.; et al. The ERA-Interim reanalysis: Configuration and performance of the data assimilation system. *Q. J. R. Meteorol. Soc.* **2011**, *137*, 553–597. [[CrossRef](#)]
30. Kohonen, T.; Hynninen, J.; Kangas, J.; Laaksonen, J. SOM_PAK: The self-organizing map program package. *Espoo Helsinki Univ. Technol. Lab. Comput. Inf. Sci.* **1996**, *1*, 39–40.
31. MacQueen, J. Others some methods for classification and analysis of multivariate observations. In *Proceedings of the Fifth Berkeley Symposium on Mathematical Statistics and Probability*; University of California Press: Oakland, CA, USA, 1967; Volume 1, pp. 281–297.
32. Hewitson, B.C.; Crane, R.G. Self-organizing maps: Applications to synoptic climatology. *Clim. Res.* **2002**, *22*, 13–26. [[CrossRef](#)]
33. Liu, Y.; Weisberg, R.H.; Mooers, C.N.K. Performance evaluation of the self-organizing map for feature extraction. *J. Geophys. Res.* **2006**, *111*, C05018. [[CrossRef](#)]
34. Reusch, D.B.; Alley, R.B.; Hewitson, B.C. North Atlantic climate variability from a self-organizing map perspective. *J. Geophys. Res.* **2007**, *112*, DO2104. [[CrossRef](#)]
35. Sheridan, S.C.; Lee, C.C. The self-organizing map in synoptic climatological research. *Prog. Phys. Geogr.* **2011**, *35*, 109–119. [[CrossRef](#)]
36. Liu, Y.; Weisberg, R.H. A Review of Self-Organizing Map Applications in Meteorology and Oceanography. In *Self-Organizing Maps: Applications and Novel Algorithm Design*; Mwasiagi, J.I., Ed.; InTech: Rijeka, Croatia, 2011; pp. 253–272.
37. Kennedy, A.D.; Dong, X.; Xi, B. Cloud fraction at the ARM SGP site: reducing uncertainty with self-organizing maps. *Theor. Appl. Climatol.* **2016**, *124*, 43–54. [[CrossRef](#)]
38. Macek-Rowland, K.M. 1997 Floods in the Red River of the North and Missouri River Basins in North Dakota and Western Minnesota: U.S. Geological Survey Open-File Report; USGS: Reston, VA, USA, 1997; pp. 97–575.
39. Rannie, W. The 1997 flood event in the Red River basin: Causes, assessment and damages. *Can. Water Resour. J.* **2016**, *41*, 45–55. [[CrossRef](#)]
40. Eichler, T.; Higgins, W. Climatology and ENSO-Related Variability of North American Extratropical Cyclone Activity. *J. Clim.* **2006**, *19*, 2076–2093. [[CrossRef](#)]
41. Seager, R.; Kushnir, Y.; Nakamura, J.; Ting, M.; Naik, N. Northern Hemisphere winter snow anomalies; ENSO, NAO and the winter of 2009/10. *J. Geophys. Res.* **2010**, *37*, L14703. [[CrossRef](#)]
42. Whittaker, L.M.; Horn, L.H. Geographical and seasonal distribution of North American cyclogenesis, 1958–1977. *Mon. Weather Rev.* **1981**, *109*, 2312–2322. [[CrossRef](#)]
43. Achtor, T.H.; Horn, L.H. Spring Season Colorado Cyclones. Part I: Use of Composites to Relate Upper and Lower Tropospheric Wind Fields. *J. Clim. Appl. Meteorol.* **1986**, *25*, 732–743. [[CrossRef](#)]
44. Schultz, D.M.; Bosart, L.F.; Colle, B.A.; Davies, H.C.; Dearden, C.; Keyser, D.; Martius, O.; Roebber, P.J.; Steenburgh, W.J.; Volkert, H.; et al. Extratropical Cyclones: A Century of Research on Meteorology's Centerpiece. *Meteorol. Monogr.* **2018**, *59*, 16.1–16.56. [[CrossRef](#)]
45. Déry, S.J.; Yau, M.K. Simulation of blowing snow in the Canadian arctic using a double-moment model. *Boundary-Layer Meteorol.* **2001**, *99*, 297–316. [[CrossRef](#)]
46. Yang, J.; Yau, M.K. A new triple-moment blowing snow model. *Boundary Layer Meteorol.* **2008**, *126*, 137–155. [[CrossRef](#)]
47. Baggaley, D.G.; Hanesiak, J.M. An empirical blowing snow forecast technique for the Canadian Arctic and Prairie Provinces. *Weather Forecast.* **2005**, *20*, 51–62. [[CrossRef](#)]
48. Compo, G.P.; Whitaker, J.S.; Sardeshmukh, P.D.; Matsui, N.; Allan, R.J.; Yin, X.; Gleason, B.E.; Vose, R.S.; Rutledge, G.; Bessemoulin, P. The twentieth century reanalysis project. *Q. J. R. Meteorol. Soc.* **2011**, *137*, 1–28. [[CrossRef](#)]
49. Soden, B.J.; Held, I.M. An assessment of climate feedbacks in coupled ocean–atmosphere models. *J. Clim.* **2006**, *19*, 3354–3360. [[CrossRef](#)]
50. Rupp, D.E.; Abatzoglou, J.T.; Hegewisch, K.C.; Mote, P.W. Evaluation of CMIP5 20th century climate simulations for the Pacific Northwest USA. *J. Geophys. Res. Atmos.* **2013**, *118*, 10,884–10,906. [[CrossRef](#)]
51. Brown, R.D.; Robinson, D.A. Northern Hemisphere spring snow cover variability and change over 1922–2010 including an assessment of uncertainty. *Cryosphere* **2011**, *5*, 219–229. [[CrossRef](#)]
52. Kunkel, K.E.; Palecki, M.A.; Ensor, L.; Easterling, D.; Hubbard, K.G.; Robinson, D.; Redmond, K. Trends in twentieth-century U.S. extreme snowfall seasons. *J. Clim.* **2009**, *22*, 6204–6216. [[CrossRef](#)]

53. Kluver, D.; Leathers, D. Regionalization of snowfall frequency and trends over the contiguous United States. *Int. J. Climatol.* **2015**, *35*, 4348–4358. [[CrossRef](#)]
54. Lambert, S.J.; Fyfe, J.C. Changes in winter cyclone frequencies and strengths simulated in enhanced greenhouse warming experiments: Results from the models participating in the IPCC diagnostic exercise. *Clim. Dyn.* **2006**, *26*, 713–728. [[CrossRef](#)]
55. Catto, J.L.; Shaffrey, L.C.; Hodges, K.I. Northern Hemisphere extratropical cyclones in a warming climate in the HiGEM high-resolution climate model. *J. Clim.* **2011**, *24*, 5336–5352. [[CrossRef](#)]
56. McCabe, G.; Clark, M.; Serreze, M. Trends in Northern Hemisphere surface cyclone frequency and intensity. *J. Clim.* **2001**, *14*, 2763–2768. [[CrossRef](#)]
57. Mizuta, R.; Matsueda, M.; Endo, H.; Yukimoto, S. Future change in extratropical cyclones associated with change in the upper troposphere. *J. Clim.* **2011**, *24*, 6456–6470. [[CrossRef](#)]
58. Long, Z.; Perrir, W.; Gyakum, J.; Laprisee, R.; Caya, D. Scenario changes in the climatology of winter midlatitude cyclone activity over eastern North America and the northwest Atlantic. *J. Geophys. Res.* **2009**, *114*, D12111. [[CrossRef](#)]
59. Eichler, T.P.; Gaggini, N.; Pan, Z. Impacts of global warming on Northern Hemisphere winter storm tracks in the CMIP5 model suite. *J. Geophys. Res. Atmos.* **2013**, *118*, 3919–3932. [[CrossRef](#)]



© 2019 by the authors. Licensee MDPI, Basel, Switzerland. This article is an open access article distributed under the terms and conditions of the Creative Commons Attribution (CC BY) license (<http://creativecommons.org/licenses/by/4.0/>).